

An overview of the QCD phase diagram at finite T and μ

Jana N. Guenther^{a,b,*}

^a*CPT, Aix-Marseille Université, 163 Avenue de Luminy, 13009 Marseille, France*

^b*Theoretical particle physics, Bergische Universität Wuppertal, Gaußstraße 20, 42119 Wuppertal*

E-mail: jguenther@uni-wuppertal.de

In recent years there has been much progress on the investigation of the QCD phase diagram with lattice QCD. This talk will focus on the developments in the last few years. Especially the addition of external influences and extended ranges of T and μ yield an increasing number of interesting results, a subset of which will be discussed. Many of these conditions are important for the understanding of both the QCD transition in the early universe and heavy ion collision experiments which are conducted for example at the LHC and RHIC. This offers many exciting opportunities for comparisons between theory and experiment.

*The 38th International Symposium on Lattice Field Theory, LATTICE2021 26th-30th July, 2021
Zoom/Gather@Massachusetts Institute of Technology*

*Speaker

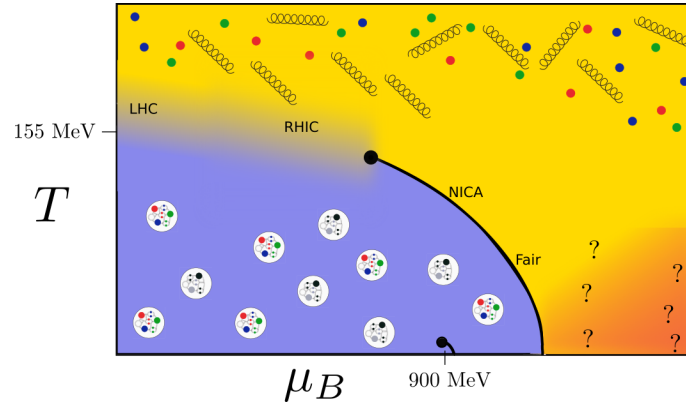


Figure 1: A schematic view on the T - μ_B -plane of the QCD phase diagram.

1. Introduction

The behaviour of QCD matter under different influences has been an active research topic for many years. The effects of different temperatures and densities are summarized in the T - μ -plane of the QCD phasediagram which is schematically displayed in figure 1. The investigation of its structure has seen significant progress in recent years both in experiments and theory.

Most experimental insights are gained from heavy ion collisions, most prominently done with gold or lead at the LHC and RHIC. Here two beams of heavy ions are collided at relativistic velocities, forming an out of equilibrium state, the so called glasma, which can be described as a color glass condensate (see for example Ref. [1, 2]). Further fragmentation into quarks and gluons lead to the quark gluon plasma. This is a state of deconfined quarks and gluons that exhibits similarities with a strongly interacting fluid and is therefore often treated in the framework of relativistic hydrodynamics. After its formation the quark gluon plasma cools down again while expanding. When the quarks and gluons, which were in a deconfined state in the quark gluon plasma, recombine to colour-neutral hadrons, the chemical abundance of the different hadron species is fixed. This is called chemical freezeout and it is assumed to take place at a similar temperature as the QCD transition. Even after the chemical freezeout, the hadrons still can exchange momentum and energy. The time when this exchange comes to a stop is called kinetic freezeout.

On the theory side, lattice QCD is an obvious tool to investigate the phase diagram. It solves QCD with controllable errors, which allows for reliable predictions. Results from QCD thermodynamics in thermal equilibrium can be obtained with high precision for vanishing chemical potential. However, the investigation of finite densities is complicated by the infamous sign problem. Other non-perturbative methods like Dyson-Schwinger-Equations or Functional Renormalization Groups do not encounter the sign problem, but fail to determine a reliable error.

Since lattice QCD simulates quantities in thermal equilibrium, the question at which states the quark gluon plasma (or the hadrons) is thermalized is very important for comparisons between experimental and lattice QCD results. The state of the glasma does not thermalize and is therefore difficult to investigate with lattice QCD.

This proceedings will focus on the review of recent progress obtained from lattice QCD. A focus will be on results with physical parameters at low finite μ_B by extrapolations from zero or

imaginary μ_B , which allow for comparisons with experimental results. Other reviews about lattice QCD results that can not be discussed here are for example Refs. [3, 4].

1.1 Extrapolation to small finite chemical potential

Since at $\mu_B = 0$ the transition is a crossover (Ref. [5–10]), some observables can be described by an analytic function in the vicinity of zero. This fact can be exploited, by using results at imaginary or zero chemical potential. A very common technique for extrapolation is the Taylor method. Within that method, the pressure is parameterized as

$$\frac{p}{T^4} = \sum_{j=0}^{\infty} \sum_{k=0}^{\infty} \frac{1}{j!k!} \chi_{jk}^{BS} \hat{\mu}_B^j \hat{\mu}_S^k \quad (1)$$

with $\hat{\mu} = \frac{\mu}{T}$. The χ_{jk}^{BS} can be measured at zero μ . Another expansion from which results will be discussed in this work, is the fugacity expansion or sector method. Here the parameterization

$$\frac{p}{T^4} = \sum_{j=0}^{\infty} \sum_{k=0}^{\infty} P_{jk}^{BS} \cosh(j\hat{\mu}_B - k\hat{\mu}_S) \quad (2)$$

is used. The expansion coefficients P_{jk}^{BS} have to be determined either from the χ_{jk}^{BS} or from imaginary chemical potential. In general, for simulations with imaginary chemical potential a wide variety of fit functions are possible to describe the data at $\mu^2 < 0$. The choice of fit function is usually guided by the fit quality, sometimes complemented by known physical insights. An advantage of the fugacity expansion is its rapid convergence in the hadronic phase and the added information on the particle content from different sectors. On the other hand, the Taylor expansion converges rapidly in the high temperature limit.

1.2 Simulations at finite chemical potential

Since the extrapolation methods discussed in section 1.1 are only feasible for small chemical potential and for an analytic transition other techniques are required to reach out further into the phase diagram. There have been many ideas around in the Lattice community how to facilitate simulations despite the sign problem, for example reweighting techniques [11–14], density of state methods [15, 16], using the canonical ensemble [17–19], formulations with dual variables [20] or Lefschetz thimbles [21, 22]. Two methods for which I will briefly discuss some recent results are Complex Langevin and Sign reweighting. While none of the available results are at physical quark masses and continuum extrapolated, and might still have some other caveats that prevent them from giving final answers on the phase diagram, impressive progress has been made recently.

Complex Langevin One way to simulate QCD with finite density, that has been intensely studied and made significant progress over recent years is to employ Complex Langevin equations. While here only a few recent results will be discussed, a more comprehensive overview can be found in Ref. [23]. Complex Langevin simulation extends the gauge group from $SU(3)$ to $SL(3, \mathbb{C})$. The non-compact nature of $SL(3, \mathbb{C})$ can lead to so called runaway configurations. To make sure the evolution stays close to the unitary manifold, which produces the correct result, gauge cooling (Refs. [24, 25]) can be employed. Other methods for improvement are the use of an adaptive step

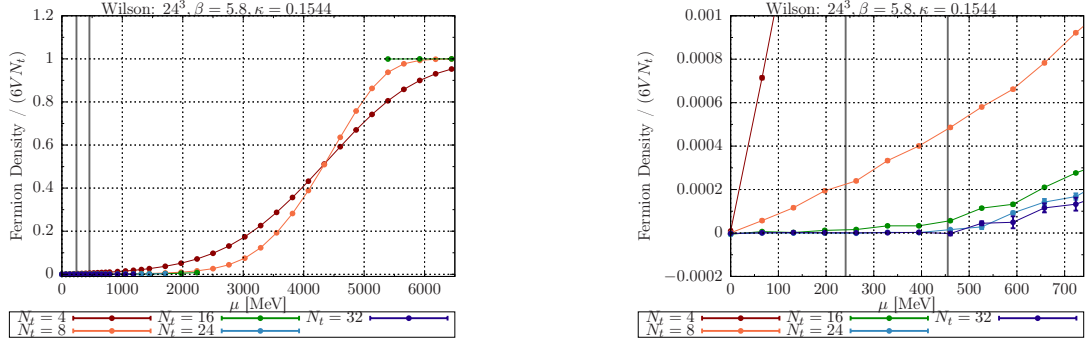


Figure 2: (Ref. [39]) The fermion density at finite chemical potential from Complex Langevin simulations. Left: Overview over a large range of chemical potential. Right: Zoom in of the lower left corner of the right side.

size for the numerical integration (Ref. [26]) and the addition of a force term to the evolution (Ref. [27]). The correctness of the result can be monitored by checking the fall-off of specific observables, which usually is required to meet a certain speed (Refs. [28–33]).

Recent results on the phase diagram with Complex Langevin simulations include the use of improved actions like the Symanzik improved gauge action and the comparison to results from the Taylor expansion method (see section 1.1) which was done in Ref. [34] with four flavors of staggered quarks with pion masses between 500 MeV and 700 MeV on $16^3 \times 8$ lattices.

Also, for heavy pions with a mass of about 1.3 GeV and two flavors of Wilson fermions the transition temperature at finite μ was computed in (Ref. [35]). The determination of the transition temperature was obtained from the third order Binder cumulant of two different observables, both related to the Polyakov loop.

In Ref. [36–38] Complex Langevin simulations in small boxes with sizes of $8^3 \times 16$ and $16^3 \times 8$ with four flavors and a lattice spacing of $a^{-1} \approx 4.7$ GeV were performed. For the dependence of the quark number on the chemical potential a plateau was observed that the authors relate to the Fermi surface and color superconductivity.

Results for a large range of chemical potentials and several lattice spacings and volumes were presented at this year’s lattice conference (Ref. [39]). Here two flavors of Wilson fermions ($m_\pi = 550$ MeV) were used for simulations of chemical potentials up to 5 GeV. The results for fermion density normalized by a factor of $\frac{1}{6VN_t}$ are shown in figure 2. They are shown for lattices with $N_s = 24$ and five different values of N_t between 4 and 32. For large chemical potential a saturation effect can be observed. For the simulations, adaptive step size scaling, gauge cooling and dynamic stabilisation were employed. The results still have to be extrapolated to a Langevin step size of zero.

Rewighting A common challenge when reweighting from zero to finite chemical potential is the overlap problem: The amount of configurations obtained by importance sampling that contain information on finite μ physics is prohibitively small because they are only in the tails of the probability distribution. To mitigate this overlap problem one can reweight from a theory where the reweighting factors are from a compact space. Two possible choices, for which results were presented at this conference (Ref. [40]), are the phase quenched theory, where the reweighting factors

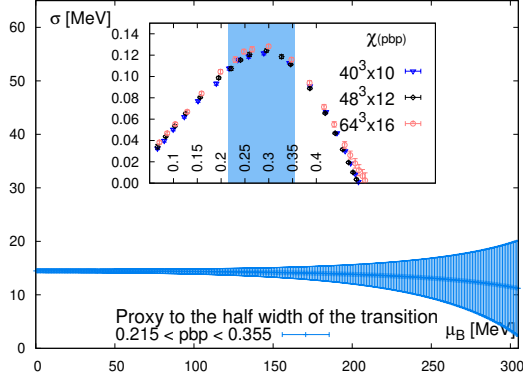


Figure 3: (Ref. [47]) Extrapolation of the half width of the transition to finite baryon chemical potential as defined in equation (3). The insert shows the chiral susceptibility χ as a function of the chiral condensate $\langle \bar{\psi}\psi \rangle$. The shaded region illustrates $\langle \bar{\psi}\psi \rangle_c \pm \Delta \langle \bar{\psi}\psi \rangle / 2$.

are pure phases $e^{i\theta}$ and the sign quenched theory (Refs. [17, 41, 42]), which also has a weaker sign problem. New results from this reweighting techniques were presented in Refs. [40, 43] for lattice with $N_t = 4$ and 6.

2. The transition temperature

The crossover nature of the transition and its temperature has been determined since 2006 with a variety of observables (Ref. [5–10, 44, 45]). More recently the transition temperature has been determined with increased precision in Ref. [46] and Ref. [47]. Often different definitions yield consistent results within the available precision. However for an analytic transition this is not guaranteed in contrast to the situation of a phase transition.

A high precision determination of the transition temperature at $\mu_B = 0$ from five different observables was done in Ref. [48]. All five definitions have the same continuum limit within the available precision. This yields a combined value of $T_c = (156 \pm 1.5)$ MeV.

A new definition as the peak of the chiral susceptibility as a function of the chiral condensate (instead of the more common definition as function of the temperature) was introduced in Ref. [47]. It allows for a more precise extraction of the transition temperature and, therefore, for an improvement in the extrapolation (see section 2.3).

By now the error on the transition temperature at $\mu_B = 0$ is much smaller than the width σ of the crossover. It has to be determined separately and is not encompassed by the error of the transition temperature. A possible definition, that has been used in Ref. [47], is

$$\langle \bar{\psi}\psi \rangle(T_c \pm \sigma/2) = \langle \bar{\psi}\psi \rangle_c \pm \Delta \langle \bar{\psi}\psi \rangle / 2. \quad (3)$$

The result, extrapolated to the continuum from three lattice spacings, can be seen in figure 3 up to $\mu_B = 300$ MeV.

2.1 Influence of many colors

On possible influence on the transition temperature is the number of colors. The large color limit is theoretically interesting as it simplifies certain aspects of QCD (see for example [49–51]).

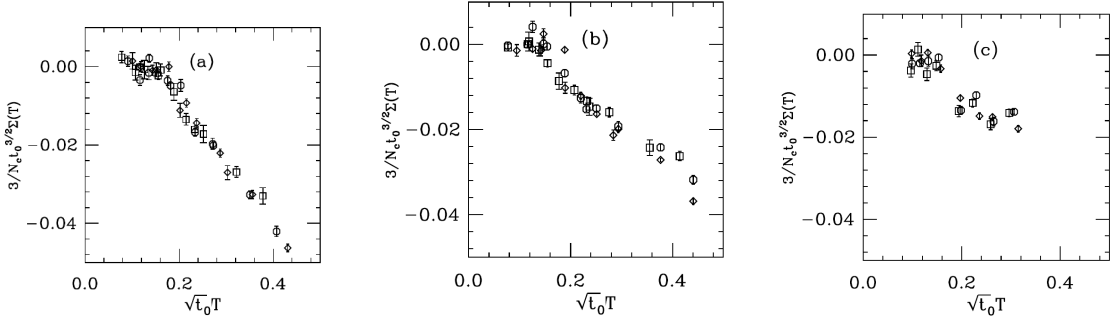


Figure 4: (Ref. [54]) The rescaled chiral condensate as a function of the temperature in units of t_0 . The number of colors is shown by the shapes: Squares: $N_c = 3$, octagons: $N_c = 4$ and diamonds: $N_c = 5$. The three plots show different pseudo scalar masses: (a) $(m_{PS}/m_V)^2 \sim 0.63$; (b) $(m_{PS}/m_V)^2 \sim 0.5$; (c) $(m_{PS}/m_V)^2 \sim 0.25$.

Recent reviews for lattice QCD with $N_c > 3$ can be found in Refs. [52, 53]. At this conference the results of Ref. [54] were presented (Ref. [55]). This work investigates T_c with $N_f = 2$ Wilson-Clover fermions for $N_c = 3, 4$ and 5. Figure 4 shows the temperature dependence of the rescaled chiral condensate for three different pseudo scalar masses. After including the rescaling factor $\frac{3}{N_c}$, the chiral condensate is within the available precision independent of the number of colors.

2.2 Quark masses and the Columbia plot

An important influence on the QCD transition temperature is its dependence on the light and strange quark masses. The Columbia plot (figure 5) shows one possible scenario for the dependence of the order of the transition as a function of the quark masses for $N_f = 2 + 1$. The infinite quark mass limit (the upper right corner) yields pure $SU(3)$ -gauge theory with static quarks where the QCD transition is of first order. When the quark masses become finite, the first order transition is getting weaker until it becomes a second order transition. On the opposite corner of the Columbia plot (the lower left corner) the chiral limit for three flavours is expected to be a first order transition as well. Again, when quark masses become larger the transition weakens until it becomes a second order transition. The limiting second order lines for both corners are still under active investigation. Several results on the Columbia plot were presented at this years lattice conference, and are roughly depicted on the right side of figure 5. However, a dedicated review of, especially the chiral limit is given in Ref. [56, 57] and not part of this proceedings.

2.3 Extrapolation to finite μ_B

The behaviour of the transition temperature in the μ_B - T -plane can be parameterized by the Taylor expansion as

$$\frac{T_c(\mu_B)}{T_c(0)} = 1 - \kappa_2 \left(\frac{\mu_B}{T_c} \right)^2 - \kappa_4 \left(\frac{\mu_B}{T_c} \right)^4 + O(\mu_B^6). \quad (4)$$

The odd powers of $\frac{\mu_B}{T}$ vanish due to the isospin symmetry. The coefficients κ_2 has been determined in several computations. The more recent ones from Refs. [46, 47, 64–66] are compared in figure 6. The green points were obtained from extrapolations with imaginary chemical potential while the

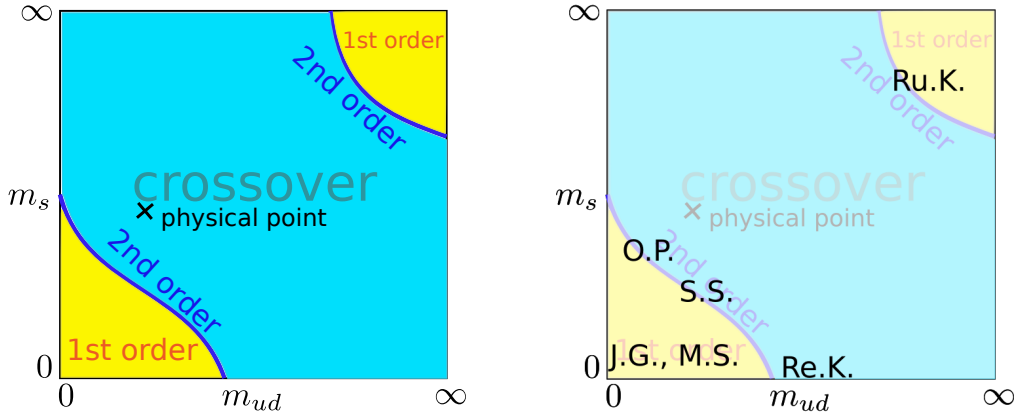


Figure 5: A schematic view of one possible version of the Columbia. On the left side the talks at this year's Lattice conference are noted as well (Refs [58–63]).

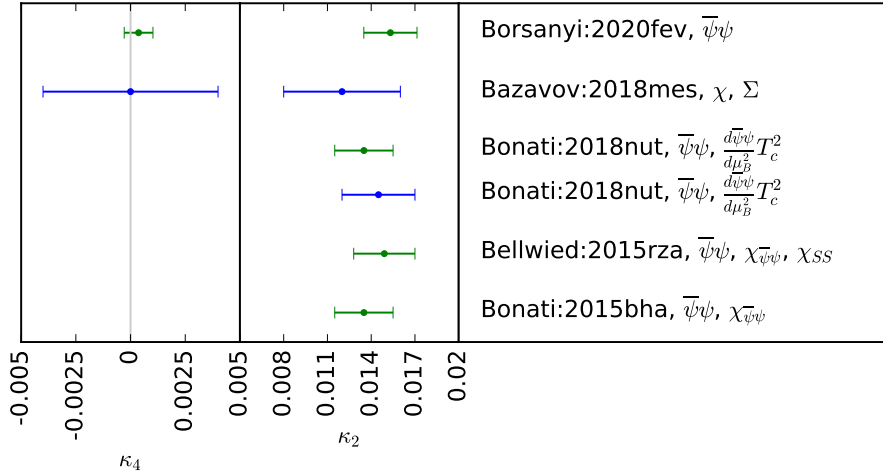


Figure 6: (Ref. [47]) Overview of the different determinations of the κ_2 and κ_4 coefficients as defined in equation (4). The values are taken from Ref. [46, 47, 64–66]. Green points correspond to determinations from imaginary chemical potential, while results shown in blue were obtained by the Taylor method.

blue points were obtained by the Taylor method. Both methods yield compatible results. In addition to κ_2 new results for κ_4 are available from Refs. [46, 47]. While it is clear that $\kappa_4 \ll \kappa_2$ the relative error of κ_4 is more than 100% and the sign is therefore still undetermined.

The extrapolation of the transition temperature to finite μ_B for the choice of vanishing net strangeness ($n_S = 0$) and $n_Q = 0.4n_B$, to match the condition in heavy ion collisions from Refs. [46, 47] is shown in figure 7. The results from Ref. [46] (left side of figure 7) rely on the Taylor expansion method. They were obtained with HISQ quarks and continuum extrapolated from three lattices with temporal extent $N_t = 6, 8, 12$.

The results on the right hand side of figure 7 were obtained from simulations at imaginary chemical potential. They are continuum extrapolated from three lattices with sizes $40^3 \times 10, 48^3 \times 12$ and $64^3 \times 16$ and obtained using stout smeared staggered quarks. The extrapolation was done with

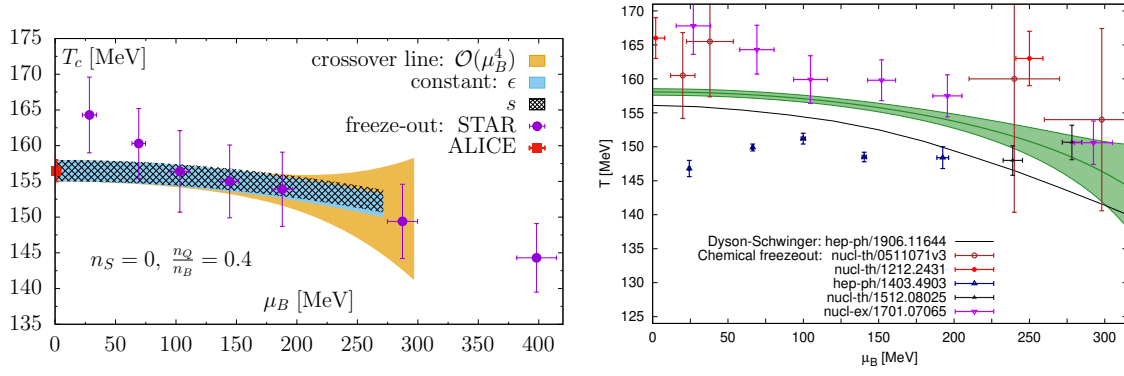


Figure 7: Left: (Ref. [46]) The extrapolation of the transition from the Taylor method compared with the freeze out temperatures from Ref. [67, 68], Right: (Ref. [47]) A comparison of the extrapolated transition temperature from simulations at imaginary chemical potential (green band) and Dyson-Schwinger-Equations (Ref. [69]). In addition the freeze-out temperatures obtained from heavy ion collisions in Ref. [70–74] are shown.

two different functions,

$$T_c = 1 + \hat{\mu}_B^2 \left(a + \frac{d}{N_t^2} \right) + \hat{\mu}_B^4 \left(b + \frac{e}{N_t^2} \right) + \hat{\mu}_B^6 \left(c + \frac{f}{N_t^2} \right) \quad (5)$$

and

$$T_c = \frac{1}{1 + \hat{\mu}_B^2 \left(a + \frac{d}{N_t^2} \right) + \hat{\mu}_B^4 \left(b + \frac{e}{N_t^2} \right) + \hat{\mu}_B^6 \left(c + \frac{f}{N_t^2} \right)} \quad (6)$$

to estimate the systematic error from the choice of extrapolation function.

As a comparison with the lattice result several data points for the freeze-out temperature (Refs. [67, 68, 70–74]) are shown. While the chemical freeze-out is not the same as the QCD transition, it is expected to occur at a similar temperature, which makes an comparison interesting. In addition, on the right side, a result from Dyson-Schwinger-Equation calculations (Ref. [69]) is shown. The curvature agrees well with the lattice result, while in that case the absolute value was set to a previous lattice value, which was determined by a different observable and with a larger error. Therefore the difference does not imply a contradiction between the two calculations.

2.4 The influence of a magnetic field

When considering the situation in heavy ion colliders, another important influence on the transition temperature is the magnetic field (Refs. [75–77]). In the last decade the simulation of QCD with a magnetic field on the lattice has been a very active field (e.g. Refs. [78–87]). In several works, which were not yet continuum extrapolated, an increase of the transition temperature with the addition of a magnetic field was found. This agreed well with the expectation resulting from the so-called magnetic catalysis, which describes that at zero temperature the chiral symmetry breaking increases with the magnetic field. However, continuum extrapolated results find the opposite behaviour, the so called inverse magnetic catalysis. Studies with various pion masses (Refs. [85, 88]) suggest that this effect is related to the deconfinement rather than the chiral

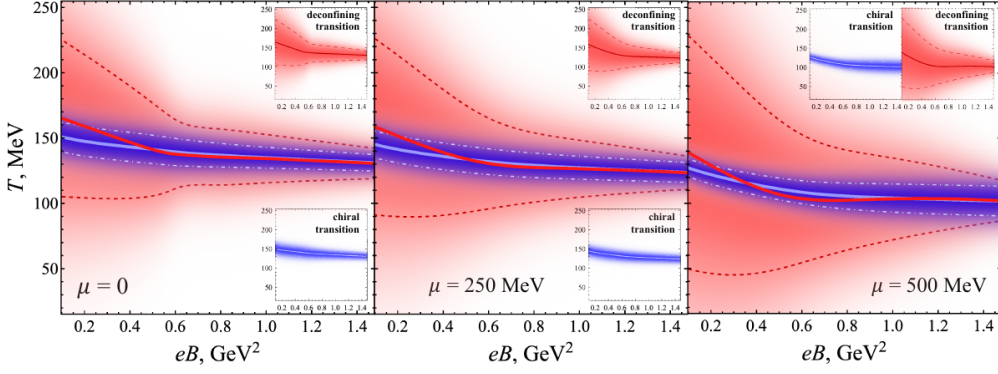


Figure 8: (Ref. [97]) The transition temperature, both for the chiral and deconfinement transition, as a function of the magnetic field, for three finite densities.

transition. The effects of a magnetic field remained an active topic at this year's lattice conference [87, 89–96]. In addition to studying a magnetic field at zero or finite temperature, now also the combination of a magnetic field and a finite density is under active investigation (Refs. [89, 90, 97]). Figure 8 shows the transition temperature, both for the chiral and deconfinement transition, as a function of the magnetic field, for three chemical potentials ($\mu_B = 0$ MeV, 250 MeV, 500 MeV). The results were obtained on $N_t = 6$ lattices with staggered quarks. They show that the addition of a chemical potential further decreases the transition temperature, which matches the expectation from extrapolation to finite density without a magnetic field (see section 2.3)

3. Fluctuations

Fluctuations are computed as the derivatives of the pressure with respect to various chemical potentials:

$$\chi_{i,j,k}^{B,Q,S} = \frac{\partial^{i+j+k}(p/T^4)}{(\partial\hat{\mu}_B)^i(\partial\hat{\mu}_Q)^j(\partial\hat{\mu}_S)^k}, \quad \hat{\mu}_i = \frac{\mu}{T} \quad (7)$$

While fluctuations to various order have previously published for example in Ref. [98–102], now new continuum extrapolated results are available in Ref. [103]. These results are obtained by the Taylor method and continuum extrapolated from lattices with $N_t = 6, 8, 12$ and 16 with HISQ fermions. The precision of these results is high enough to allow for a comparison to different models with detailed studies for example on inclusion or exclusion of various states in a Hadron Resonance Gas model, as shown figure 9. To match the lattice results, for example for χ_{11}^{BS} , it is necessary to add states from quark models to the list of resonances from the PDG [104].

On the other hand in Refs [105, 106] results on the fugacity expansion coefficients (see equation (2)) from imaginary chemical potential are presented. Here the results are continuum estimates obtained with stout smeared staggered fermions on $N_t = 8, 10$ and 12 lattices. The analysis is based on a two dimensional fugacity expansion with imaginary μ_B and μ_S . The result for P_{21}^{BS} is shown in figure 10. This coefficient includes contributions from $N - \Lambda$ and $N - \Sigma$ scattering. The negative trend indicates the presence of a repulsive interaction that cannot be described with the addition of more resonances.

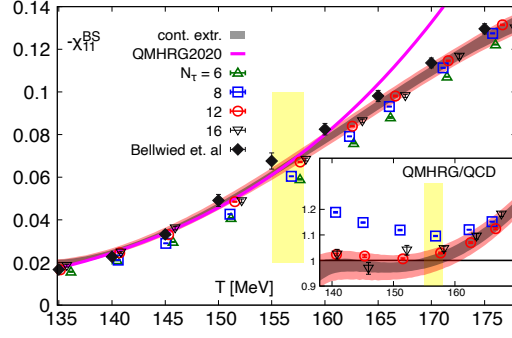


Figure 9: (Ref. [103]) New continuum extrapolated results ($N_t = 6, 8, 12, 16$) allow for detailed comparisons with various models.

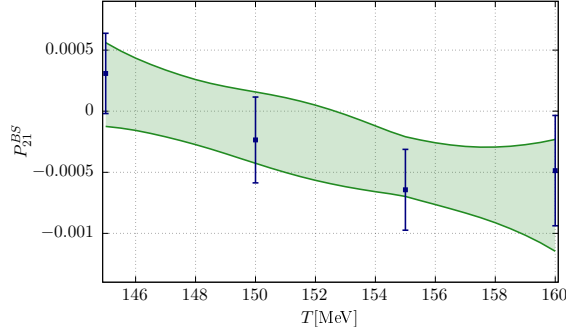


Figure 10: (Ref. [105]) Continuum estimate for the fugacity expansion coefficient (see equation (2)) from $N_t = 8, 10, 12$ with stout smeared staggered fermions. This coefficient includes contributions from $N - \Lambda$ and $N - \Sigma$ scattering. The negative trend indicates the presence of a repulsive interaction that cannot be described with the addition of more resonances.

The ratios of various fluctuations can be used to express the cumulants of the Baryon number distribution. This offers an observable for comparisons with heavy ion collision measurements of the proton number distribution. At the current precision level this can only be a rough comparison. If the precision is increased in the future, other effects should be taken into account, like the continuum limit on the lattice side, or volume fluctuations and on equilibrium effects on the experimental side.

Figure 11 from Ref. [102] shows the ratios

$$R_{31}^B(T, \mu_B) = \frac{\chi_3^B}{\chi_1^B} = \frac{S_B \sigma_B^3}{M_B} \quad (8)$$

$$R_{42}^B(T, \mu_B) = \frac{\chi_4^B}{\chi_2^B} = \kappa_B \sigma_B^2 \quad (9)$$

$$R_{51}^B(T, \mu_B) = \frac{\chi_5^B}{\chi_1^B} \quad (10)$$

$$R_{62}^B(T, \mu_B) = \frac{\chi_6^B}{\chi_2^B} \quad (11)$$

as a function of $R_{12}^B(T, \mu_B) = \frac{M_B}{\sigma_B^2}$ evaluated along the transition line. Here M_B , σ_B^2 , S_B and κ_B

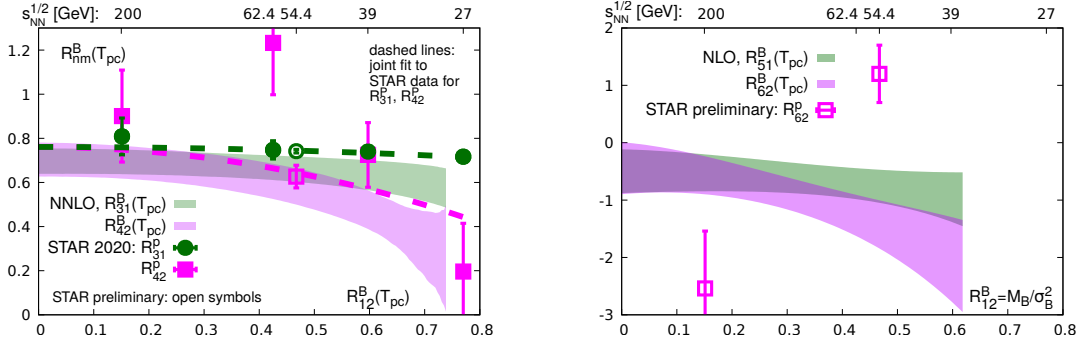


Figure 11: (Ref. [102]) Left: The ratios $R_{31}^B(T, \mu_B) = S_B \sigma_B^3 / M_B$ and $R_{42}^B(T, \mu_B) = \kappa_B \sigma_B^2$ as a function of $R_{12}^B(T, \mu_B) = M_B / \sigma_B^2$ evaluated along the transition line in comparison to the data from the STAR collaboration (Ref. [107, 108]). Right: The ratios $R_{51}^B(T, \mu_B)$ and $R_{62}^B(T, \mu_B)$ as a function of $R_{12}^B(T, \mu_B)$ in comparison to the data from the STAR collaboration (Ref. [108]).

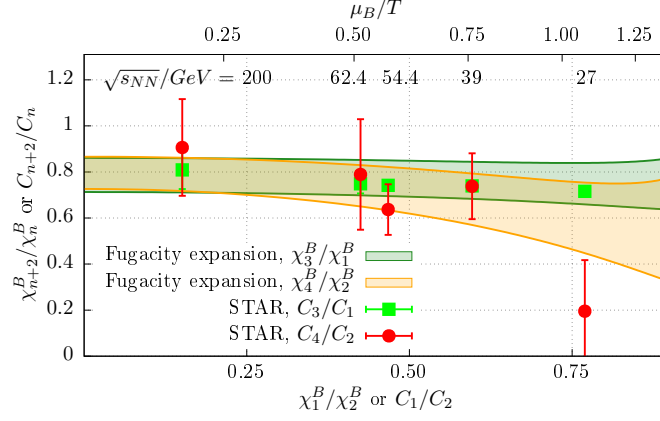


Figure 12: (Ref. [105]) The ratios $R_{31}^B(T, \mu_B) = S_B \sigma_B^3 / M_B$ and $R_{42}^B(T, \mu_B) \equiv \kappa_B \sigma_B^2$ as a function of $R_{12}^B(T, \mu_B) = M_B / \sigma_B^2$ evaluated along the transition line in comparison to the data from the STAR collaboration (Ref. [107]).

refer to the first four cumulants of the net baryon number distribution (mean, variance, skewness and kurtosis). While the two lower order ratios are a continuum estimate from $N_t = 8$ and $N_t = 12$ lattices, $R_{51}^B(T, \mu_B)$ and $R_{62}^B(T, \mu_B)$ are computed only on an $N_t = 8$ lattice. A corresponding result from Ref. [105], which has already been discussed above, is shown in figure 12.

To include strange particles like K or Λ in the comparison with lattice calculations, suitable observables have to be constructed. Ref. [109] used the Hadron Resonance Gas (HRG) model to compare different proxies (see left of figure 13). The proxy $\sigma_\Lambda^2 / (\sigma_\Lambda^2 + \sigma_K^2)$ for the fluctuation ratio $-\frac{\chi_{11}^{BS}}{\chi_2^S}$ was further investigated both by comparing the HRG and the experimental (see middle of figure 13) results, as well as lattice calculations from both the Taylor and sector method (see right of figure 13).

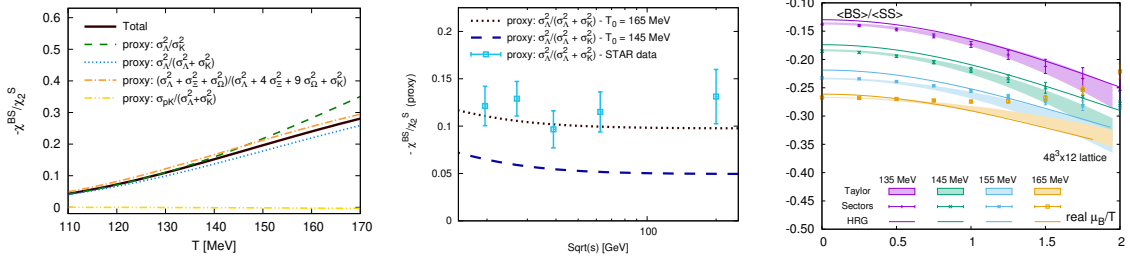


Figure 13: (Ref. [109]) Left: Calculations for different combinations of particle number cumulants (proxies) that could be measurable in heavy ion collision experiments and the total of $-\frac{\chi_{11}^{BS}}{\chi_2^S}$ that is accessible in lattice QCD calculations with the Hadron Resonance Gas (HRG) model. Middle: Comparison of the proxy $\sigma_\Lambda^2/(\sigma_\Lambda^2 + \sigma_K^2)$ for two temperatures in the HRG model and experimental results from Ref. [110] Right: Comparison between the Taylor (see equation (1)) and the sector (see equation (2)) method for $-\frac{\chi_{11}^{BS}}{\chi_2^S}$ on an $48^3 \times 12$ lattice, as well as results from the HRG model.

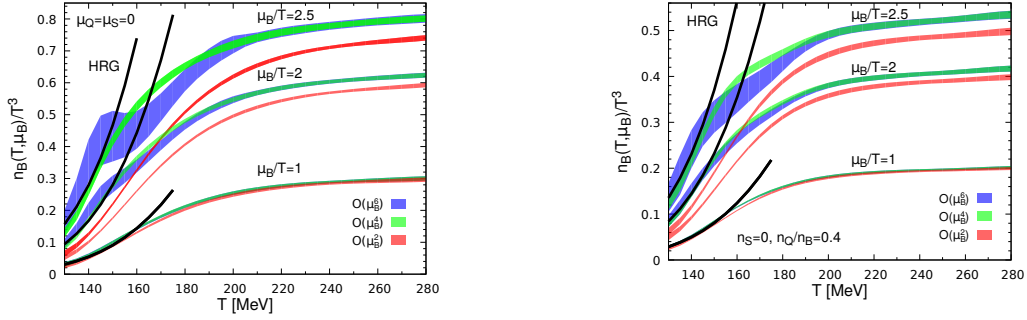


Figure 14: (Ref. [100]) The extrapolation to finite baryon number n_B done by the Taylor method (see equation (1)): Left: $\mu_Q = \mu_S = 0$, Right: $n_S = 0$ and $n_Q/n_B = 0.4$

4. The equation of state

Another quantity that has been investigated for long time is the equation of state. In the following some progress on the baryon number n_B will be discussed. When extrapolated to finite μ_B with a Taylor expansion up to μ_B^6 it shows an increase in the error around the transition temperature, which leaves room for unexpected behavior. (see figure 14 and top row of figure 15). This has been observed by different groups and on different data sets (Refs. [100, 111]). In Ref. [111] a simple toy model suggest that this behavior could be linked to the cut-off in the Taylor series in this region, which is illustrated in the bottom row of figure 15. A possible explanation for the extra challenges around the transition temperature might be that the extrapolation has to cover both the hadronic and the quark gluon plasma phase. Therefore a new extrapolation scheme from imaginary μ_B was proposed that shows a smooth behaviour as can be seen in figure 16. Now the inclusion of an extra term does increase the error more broadly over all temperatures. This behavior can make the results more suitable, if the lattice results are taken as input in hydrodynamic models, where often only the central value is used.

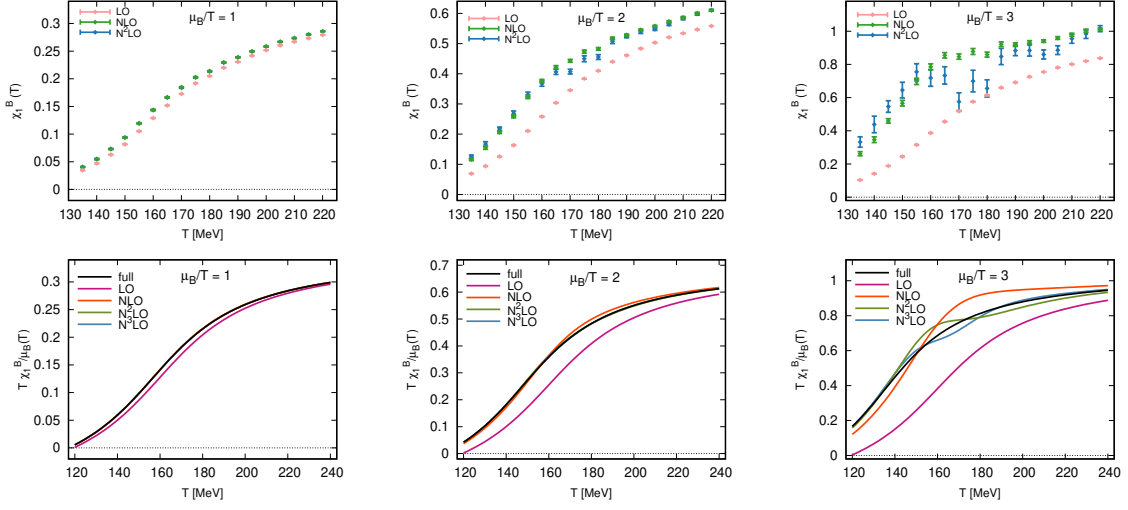


Figure 15: (Ref. [111]) Top row: The extrapolation of χ_1^B with data from Ref. [101] on $N_t = 12$ lattices to different chemical potentials. Bottom row: The same extrapolation in a simple toy model with different orders of the Taylor expansion.

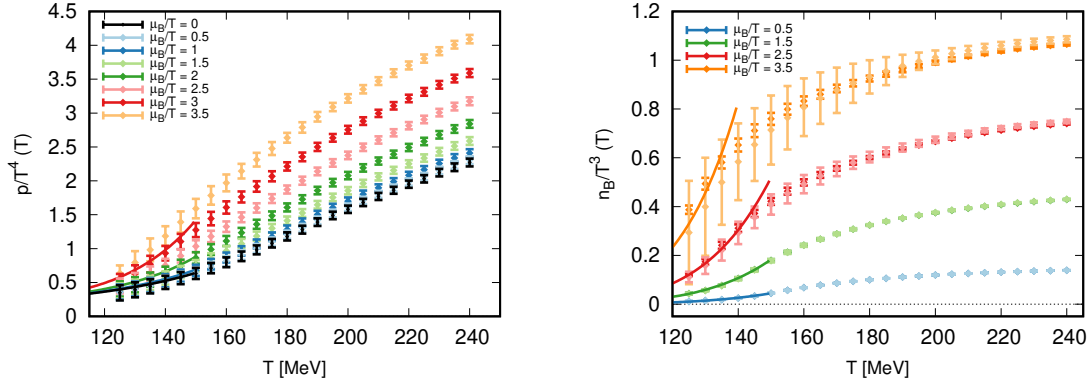


Figure 16: (Ref. [111]) The pressure and the baryon number from the resummed extrapolation. The lighter bars show the increased error by the inclusion of a higher order term.

5. The critical endpoint

The most sought after point in the QCD phase diagram is the critical endpoint, where the analytical transition between quark gluon plasma and hadrons becomes second order. However a comprehensive determination of the point is highly challenging. In this section I will briefly discuss three different ansatzes that can lead to some insight despite all the challenges.

5.1 Lee-Yang edge singularities

One way to search for a critical endpoint in the QCD phase diagram is to look for Lee-Yang edge singularities (Ref. [112]). There have been recent efforts (Refs. [42, 113, 114]) to use reweighing to determine the leading singularities in the complex plane. New results presented at this years lattice conference use the fluctuations χ_1^B , χ_2^B and χ_3^B to find a rational approximation for this quantities.

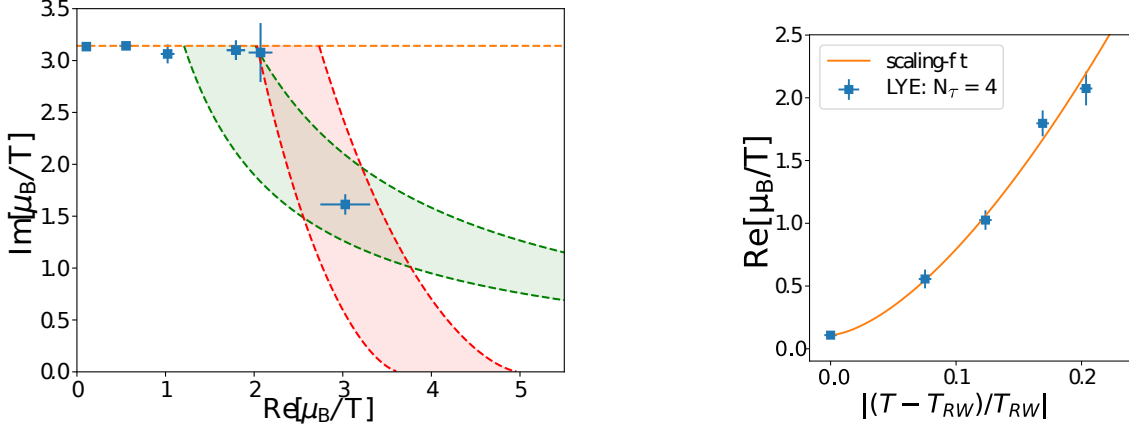


Figure 17: (Ref. [114, 115]) Blue points: Results for Lee-Yang edge singularities from $N_t = 4$ and 6 lattices. Left: Position of Lee-Yang edge singularities in the complex plane. Shaded areas show the expected areas for the Roberge-Weiss ($Z(2)$) in orange, the chiral ($O(4)/O(2)$) in green and the critical endpoint ($Z(2)$) in red. Right: The scaling fit of the Lee-Yang edge singularities associated with the Roberge-Weiss critical endpoint. The shaded areas are extracted from the expected scaling behavior that is stated for each critical endpoint.

This approximation can then be used to determine the Lee-Yang edge singularities by solving for the zeros of the polynomial in the denominator. The simulation were done with 2+1-flavors of HISQ quarks on lattices with $N_t = 4$ and 6 and shown in figure 17. On the left side shaded areas are extracted from the expected scaling behavior of different critical endpoints: The first one is the Roberge-Weiss critical endpoint which is accessible from direct simulations at imaginary chemical potential. The second one is the chiral critical endpoint which is discussed in section 2.2. The third one is the QCD critical endpoint. Most singularities that could be determined seem to correspond to the Roberge-Weiss transition, for which the scaling behavior is shown on the right side of figure 17.

5.2 Universality

An important feature of a second order phase transition is the universality in its vicinity. This would allow to extract information about the QCD phase diagram by studying different theories or models, which can be more accessible compared to full QCD at finite density. To make this possible the universality class and a mapping between QCD and the theory under investigation has to be established. Results of one possible model were presented at this years lattice conference (Refs. [116, 117]). In Ref. [118] a \mathcal{PT} symmetric quark model with $Z(2)$ symmetry was studied. Its action is given as

$$S(\phi, \chi) = \sum_x \frac{1}{2} (\nabla_\mu \phi)^2 + \frac{1}{2} (\nabla_\mu \chi)^2 + V(\phi, \chi) \quad (12)$$

with

$$V(\phi, \chi) = \frac{1}{2} m_\chi^2 \chi^2 - ig \phi \chi + U(\phi) + h \phi. \quad (13)$$

Around the chritical endpoint pattered regions are found, which the authors compare to the patterns of nuclear pasta (see e.g. Ref. [119]). In figure 18 the phase diagram for this model is shown.

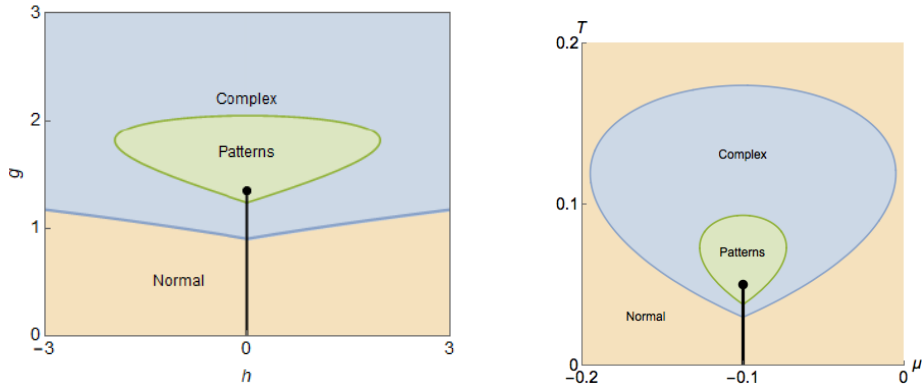


Figure 18: (Ref. [117, 118]) Patterns around a critical endpoint in a QCD-inspired heavy quark model.

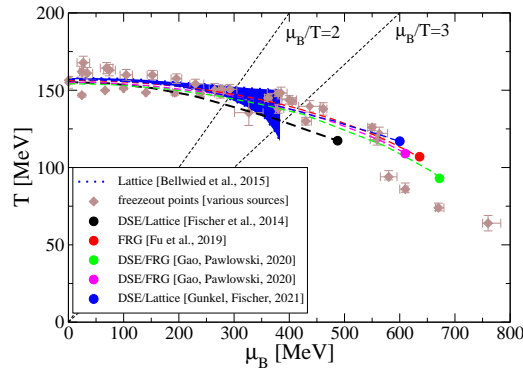


Figure 19: (Ref. [132]) Overview over results on the QCD transition line from Lattice QCD, FRG and DSE (Refs. [65, 121, 129, 133–135]), as well as results on the freeze-out line from heavy ion collision experiment.

5.3 Functional methods

Another approach, beside lattice QCD, to study QCD from its fundamental degrees of freedom are the functional methods. Under this name, both Functional Renormalization group (FRG) (see e.g. Refs. [120–125]) and Dyson-Schwinger equations (DSE) (see e.g. Refs. [69, 126–129, 129, 130]) are combined. DSE rely on an infinite tower of equations that give an exact representation of QCD. However to solve those equations this tower has to be truncated, which introduces an error that cannot be estimated at the moment. The FRG method relies on a functional integro-differential equation to describe the flow of the action (Ref. [131]). Again a truncation introduces an unknown error. An idea for an error estimation can be gained from the comparison between different truncations, methods or with lattice and experimental results. An overview over some recent determinations of the crossover line in the QCD phase diagram and the critical endpoint in comparison with lattice and freeze-out results can be seen in figure 19. The newer computations agree well with the lattice results and the critical endpoint estimations seem to be concentrated in an relative small part of the phase diagram. However further investigation and comparison of other observables is necessary before any conclusions can be drawn.

6. Conclusion

As was evident at this conference, the QCD phase diagram is a very active topic of research with lots of exciting challenges for lattice QCD. The understanding of the phase diagram is a fascinating subject for theory and experiments. In addition, with new experimental results expected in the next years, further progress in theory is needed to be able to give input and enable comparisons as close to the experimental conditions as possible. This proceedings tried to update and add on last year's review (Ref. [4]) with a focus on activities at the conference. Still, not all aspects could be discussed. For example, another axis of the phase diagram, for which new results are available, is the dependence on the isospin chemical potential (Refs. [136–138]). For many aspects the next years promise to be interesting, with the hope of new insights and understanding in various areas.

Acknowledgments

The project leading to this publication has received funding from Excellence Initiative of Aix-Marseille University - A*MIDEX, a French “Investissements d’Avenir” programme, AMX-18-ACE-005. Several of the projects discussed here also received support from the BMBF Grant No. 05P18PXFCA. This proceeding is part of a project that has received funding from the European Union’s Horizon 2020 research and innovation program under grant agreement STRONG – 2020 - No 824093. The author gratefully acknowledges the Gauss Centre for Supercomputing e.V. (www.gauss-centre.eu) for funding several projects, which are part of this review, by providing computing time on the GCS Supercomputer HAWK at HLRS, Stuttgart. The author thanks Lukas Varnhorst for proofreading and discussion.

References

- [1] F. Gelis, E. Iancu, J. Jalilian-Marian and R. Venugopalan, *The Color Glass Condensate*, *Ann. Rev. Nucl. Part. Sci.* **60** (2010) 463 [[1002.0333](#)].
- [2] F. Gelis, *Color Glass Condensate and Glasma*, *Int. J. Mod. Phys. A* **28** (2013) 1330001 [[1211.3327](#)].
- [3] O. Philipsen, *Constraining the QCD phase diagram at finite temperature and density*, *PoS LATTICE2019* (2019) 273 [[1912.04827](#)].
- [4] J.N. Guenther, *Overview of the QCD phase diagram: Recent progress from the lattice*, *Eur. Phys. J. A* **57** (2021) 136 [[2010.15503](#)].
- [5] Y. Aoki, G. Endrodi, Z. Fodor, S.D. Katz and K.K. Szabo, *The Order of the quantum chromodynamics transition predicted by the standard model of particle physics*, *Nature* **443** (2006) 675 [[hep-lat/0611014](#)].
- [6] Y. Aoki, Z. Fodor, S. Katz and K. Szabo, *The QCD transition temperature: Results with physical masses in the continuum limit*, *Phys. Lett. B* **643** (2006) 46 [[hep-lat/0609068](#)].

- [7] Y. Aoki, S. Borsanyi, S. Durr, Z. Fodor, S.D. Katz, S. Krieg et al., *The QCD transition temperature: results with physical masses in the continuum limit II.*, *JHEP* **06** (2009) 088 [0903.4155].
- [8] WUPPERTAL-BUDAPEST collaboration, *Is there still any T_c mystery in lattice QCD? Results with physical masses in the continuum limit III*, *JHEP* **09** (2010) 073 [1005.3508].
- [9] T. Bhattacharya et al., *QCD Phase Transition with Chiral Quarks and Physical Quark Masses*, *Phys. Rev. Lett.* **113** (2014) 082001 [1402.5175].
- [10] A. Bazavov et al., *The chiral and deconfinement aspects of the QCD transition*, *Phys. Rev. D* **85** (2012) 054503 [1111.1710].
- [11] I.M. Barbour, S.E. Morrison, E.G. Klepfish, J.B. Kogut and M.-P. Lombardo, *Results on finite density QCD*, *Nucl. Phys. B Proc. Suppl.* **60** (1998) 220 [hep-lat/9705042].
- [12] Z. Fodor and S.D. Katz, *A New method to study lattice QCD at finite temperature and chemical potential*, *Phys. Lett.* **B534** (2002) 87 [hep-lat/0104001].
- [13] Z. Fodor and S.D. Katz, *Lattice determination of the critical point of QCD at finite T and μ* , *JHEP* **03** (2002) 014 [hep-lat/0106002].
- [14] F. Csikor, G. Egri, Z. Fodor, S. Katz, K. Szabo and A. Toth, *The QCD equation of state at finite T and μ* , *Nucl. Phys. B Proc. Suppl.* **119** (2003) 547 [hep-lat/0209114].
- [15] Z. Fodor, S.D. Katz and C. Schmidt, *The Density of states method at non-zero chemical potential*, *JHEP* **03** (2007) 121 [hep-lat/0701022].
- [16] A. Alexandru, C. Gattringer, H.P. Schadler, K. Splittorff and J. Verbaarschot, *Distribution of Canonical Determinants in QCD*, *Phys. Rev. D* **91** (2015) 074501 [1411.4143].
- [17] A. Alexandru, M. Faber, I. Horvath and K.-F. Liu, *Lattice QCD at finite density via a new canonical approach*, *Phys. Rev. D* **72** (2005) 114513 [hep-lat/0507020].
- [18] S. Kratochvila and P. de Forcrand, *The Canonical approach to finite density QCD*, *PoS LAT2005* (2006) 167 [hep-lat/0509143].
- [19] S. Ejiri, *Canonical partition function and finite density phase transition in lattice QCD*, *Phys. Rev. D* **78** (2008) 074507 [0804.3227].
- [20] C. Gattringer, *New developments for dual methods in lattice field theory at non-zero density*, *PoS LATTICE2013* (2014) 002 [1401.7788].
- [21] L. Scorzato, *The Lefschetz thimble and the sign problem*, *PoS LATTICE2015* (2016) 016 [1512.08039].
- [22] A. Alexandru, G. Basar and P. Bedaque, *Monte Carlo algorithm for simulating fermions on Lefschetz thimbles*, *Phys. Rev. D* **93** (2016) 014504 [1510.03258].

- [23] F. Attanasio, B. Jäger and F.P. Ziegler, *Complex Langevin and the QCD phase diagram: Recent developments*, 2006.00476.
- [24] E. Seiler, D. Sexty and I.-O. Stamatescu, *Gauge cooling in complex Langevin for QCD with heavy quarks*, *Phys. Lett. B* **723** (2013) 213 [1211.3709].
- [25] G. Aarts, L. Bongiovanni, E. Seiler, D. Sexty and I.-O. Stamatescu, *Controlling complex Langevin dynamics at finite density*, *Eur. Phys. J. A* **49** (2013) 89 [1303.6425].
- [26] G. Aarts, F.A. James, E. Seiler and I.-O. Stamatescu, *Adaptive stepsize and instabilities in complex Langevin dynamics*, *Phys. Lett. B* **687** (2010) 154 [0912.0617].
- [27] F. Attanasio and B. Jäger, *Dynamical stabilisation of complex Langevin simulations of QCD*, *Eur. Phys. J. C* **79** (2019) 16 [1808.04400].
- [28] J. Nishimura and S. Shimasaki, *New Insights into the Problem with a Singular Drift Term in the Complex Langevin Method*, *Phys. Rev. D* **92** (2015) 011501 [1504.08359].
- [29] G. Aarts, E. Seiler, D. Sexty and I.-O. Stamatescu, *Complex Langevin dynamics and zeroes of the fermion determinant*, *JHEP* **05** (2017) 044 [1701.02322].
- [30] K. Nagata, J. Nishimura and S. Shimasaki, *Argument for justification of the complex Langevin method and the condition for correct convergence*, *Phys. Rev. D* **94** (2016) 114515 [1606.07627].
- [31] K. Nagata, J. Nishimura and S. Shimasaki, *Testing the criterion for correct convergence in the complex Langevin method*, *JHEP* **05** (2018) 004 [1802.01876].
- [32] M. Scherzer, E. Seiler, D. Sexty and I.-O. Stamatescu, *Complex Langevin and boundary terms*, *Phys. Rev. D* **99** (2019) 014512 [1808.05187].
- [33] S. Tsutsui, Y. Ito, H. Matsufuru, J. Nishimura, S. Shimasaki and A. Tsuchiya, *Exploring the QCD phase diagram at finite density by the complex Langevin method on a $16^3 \times 32$ lattice*, *PoS LATTICE2019* (2019) 151 [1912.00361].
- [34] D. Sexty, *Calculating the equation of state of dense quark-gluon plasma using the complex Langevin equation*, *Phys. Rev. D* **100** (2019) 074503 [1907.08712].
- [35] M. Scherzer, D. Sexty and I.-O. Stamatescu, *Deconfinement transition line with the complex Langevin equation up to $\mu/T \sim 5$* , *Phys. Rev. D* **102** (2020) 014515 [2004.05372].
- [36] Y. Ito, H. Matsufuru, Y. Namekawa, J. Nishimura, S. Shimasaki, A. Tsuchiya et al., *Complex Langevin calculations in QCD at finite density*, *JHEP* **10** (2020) 144 [2007.08778].
- [37] Y. Namekawa, Y. Asano, Y. Ito, T. Kaneko, H. Matsufuru, J. Nishimura et al., *Flavor number dependence of QCD at finite density by the complex Langevin method*, in *38th International Symposium on Lattice Field Theory*, 11, 2021 [2112.00150].

- [38] S. Tsutsui, Y. Asano, Y. Ito, H. Matsufuru, Y. Namekawa, J. Nishimura et al., *Color superconductivity in a small box: a complex Langevin study*, in *38th International Symposium on Lattice Field Theory*, 11, 2021 [[2111.15095](#)].
- [39] F. Attanasio, B. Jäger and F.P.G. Ziegler, *With complex Langevin towards the QCD phase diagram*, in *38th International Symposium on Lattice Field Theory*, 11, 2021 [[2111.02241](#)].
- [40] A. Pasztor, S. Borsanyi, Z. Fodor, K. Kapas, S.D. Katz, M. Giordano et al., *New approach to lattice QCD at finite density: reweighting without an overlap problem*, in *38th International Symposium on Lattice Field Theory*, 12, 2021 [[2112.02134](#)].
- [41] P. de Forcrand, S. Kim and T. Takaishi, *QCD simulations at small chemical potential*, *Nucl. Phys. B Proc. Suppl.* **119** (2003) 541 [[hep-lat/0209126](#)].
- [42] M. Giordano, K. Kapas, S.D. Katz, D. Negradi and A. Pasztor, *New approach to lattice QCD at finite density; results for the critical end point on coarse lattices*, *JHEP* **05** (2020) 088 [[2004.10800](#)].
- [43] S. Borsanyi, Z. Fodor, M. Giordano, S.D. Katz, D. Negradi, A. Pasztor et al., *Lattice simulations of the QCD chiral transition at real baryon density*, [2108.09213](#).
- [44] M. Cheng et al., *The Transition temperature in QCD*, *Phys. Rev. D* **74** (2006) 054507 [[hep-lat/0608013](#)].
- [45] A. Bazavov et al., *Equation of state and QCD transition at finite temperature*, *Phys. Rev. D* **80** (2009) 014504 [[0903.4379](#)].
- [46] HOTQCD collaboration, *Chiral crossover in QCD at zero and non-zero chemical potentials*, *Phys. Lett.* **B795** (2019) 15 [[1812.08235](#)].
- [47] S. Borsanyi, Z. Fodor, J.N. Guenther, R. Kara, S.D. Katz, P. Parotto et al., *The QCD crossover at finite chemical potential from lattice simulations*, [2002.02821](#).
- [48] HOTQCD collaboration, *The QCD crossover at zero and non-zero baryon densities from Lattice QCD*, *Nucl. Phys. A* **982** (2019) 847 [[1807.05607](#)].
- [49] G. 't Hooft, *A Planar Diagram Theory for Strong Interactions*, *Nucl. Phys. B* **72** (1974) 461.
- [50] G. 't Hooft, *A Two-Dimensional Model for Mesons*, *Nucl. Phys. B* **75** (1974) 461.
- [51] E. Witten, *Baryons in the $1/n$ Expansion*, *Nucl. Phys. B* **160** (1979) 57.
- [52] M. García Pérez, *Prospects for large N gauge theories on the lattice*, *PoS LATTICE2019* (2020) 276 [[2001.10859](#)].
- [53] P. Hernández and F. Romero-López, *The large N_c limit of QCD on the lattice*, *Eur. Phys. J. A* **57** (2021) 52 [[2012.03331](#)].

- [54] T. DeGrand, *Finite temperature properties of QCD with two flavors and three, four and five colors*, *Phys. Rev. D* **103** (2021) 094513 [2102.01150].
- [55] T. DeGrand, *Funny business from the large N_c finite temperature crossover*, in *38th International Symposium on Lattice Field Theory*, 9, 2021 [2109.10337].
- [56] A. Lahiri, “Aspects of finite temperature qcd approaching the chiral limit.”
- [57] A. Lahiri, *Aspects of finite temperature QCD approaching the chiral limit*.
- [58] F. Cuteri, O. Philipsen, A. Schön and A. Sciarra, *The deconfinement critical point of lattice QCD with $N_f = 2$ Wilson fermions*, 2009.14033.
- [59] R. Kara, S. Borsanyi, Z. Fodor, J.N. Guenther, P. Parotto, A. Pasztor et al., *The upper right corner of the Columbia plot with staggered fermions*, in *38th International Symposium on Lattice Field Theory*, 12, 2021 [2112.04192].
- [60] D.A. Clarke, J. Goswami, F. Karsch, A. Lahiri, M. Neumann and C. Schmidt, *Lattice QCD at Imaginary Chemical Potential in the Chiral Limit*, in *38th International Symposium on Lattice Field Theory*, 11, 2021 [2111.15621].
- [61] L. Dini, P. Hegde, F. Karsch, A. Lahiri, C. Schmidt and S. Sharma, *The Chiral Phase Transition in 3-flavor QCD from Lattice QCD*, 2111.12599.
- [62] O. Philipsen, *Lattice Constraints on the QCD Chiral Phase Transition at Finite Temperature and Baryon Density*, *Symmetry* **13** (2021) 2079 [2111.03590].
- [63] F. Cuteri, O. Philipsen and A. Sciarra, *On the order of the QCD chiral phase transition for different numbers of quark flavours*, *JHEP* **11** (2021) 141 [2107.12739].
- [64] C. Bonati, M. D’Elia, F. Negro, F. Sanfilippo and K. Zambello, *Curvature of the pseudocritical line in QCD: Taylor expansion matches analytic continuation*, *Phys. Rev. D* **98** (2018) 054510 [1805.02960].
- [65] R. Bellwied, S. Borsanyi, Z. Fodor, J. Guenther, S.D. Katz, C. Ratti et al., *The QCD phase diagram from analytic continuation*, *Phys. Lett.* **B751** (2015) 559 [1507.07510].
- [66] C. Bonati, M. D’Elia, M. Mariti, M. Mesiti, F. Negro and F. Sanfilippo, *Curvature of the chiral pseudocritical line in QCD: Continuum extrapolated results*, *Phys. Rev.* **D92** (2015) 054503 [1507.03571].
- [67] A. Andronic, P. Braun-Munzinger, K. Redlich and J. Stachel, *Decoding the phase structure of QCD via particle production at high energy*, *Nature* **561** (2018) 321 [1710.09425].
- [68] STAR collaboration, *Bulk Properties of the Medium Produced in Relativistic Heavy-Ion Collisions from the Beam Energy Scan Program*, *Phys. Rev. C* **96** (2017) 044904 [1701.07065].

- [69] P. Isserstedt, M. Buballa, C.S. Fischer and P.J. Gunkel, *Baryon number fluctuations in the QCD phase diagram from Dyson-Schwinger equations*, *Phys. Rev.* **D100** (2019) 074011 [1906.11644].
- [70] A. Andronic, P. Braun-Munzinger and J. Stachel, *Hadron production in central nucleus-nucleus collisions at chemical freeze-out*, *Nucl. Phys.* **A772** (2006) 167 [nucl-th/0511071].
- [71] F. Becattini, M. Bleicher, T. Kollegger, T. Schuster, J. Steinheimer and R. Stock, *Hadron Formation in Relativistic Nuclear Collisions and the QCD Phase Diagram*, *Phys. Rev. Lett.* **111** (2013) 082302 [1212.2431].
- [72] P. Alba, W. Alberico, R. Bellwied, M. Bluhm, V. Mantovani Sarti, M. Nahrgang et al., *Freeze-out conditions from net-proton and net-charge fluctuations at RHIC*, *Phys. Lett.* **B738** (2014) 305 [1403.4903].
- [73] V. Vovchenko, V.V. Begun and M.I. Gorenstein, *Hadron multiplicities and chemical freeze-out conditions in proton-proton and nucleus-nucleus collisions*, *Phys. Rev.* **C93** (2016) 064906 [1512.08025].
- [74] STAR collaboration, *Bulk Properties of the Medium Produced in Relativistic Heavy-Ion Collisions from the Beam Energy Scan Program*, *Phys. Rev.* **C96** (2017) 044904 [1701.07065].
- [75] D.E. Kharzeev, L.D. McLerran and H.J. Warringa, *The Effects of topological charge change in heavy ion collisions: 'Event by event P and CP violation'*, *Nucl. Phys. A* **803** (2008) 227 [0711.0950].
- [76] V. Skokov, A. Illarionov and V. Toneev, *Estimate of the magnetic field strength in heavy-ion collisions*, *Int. J. Mod. Phys. A* **24** (2009) 5925 [0907.1396].
- [77] W.-T. Deng and X.-G. Huang, *Event-by-event generation of electromagnetic fields in heavy-ion collisions*, *Phys. Rev. C* **85** (2012) 044907 [1201.5108].
- [78] M. D'Elia, S. Mukherjee and F. Sanfilippo, *QCD Phase Transition in a Strong Magnetic Background*, *Phys. Rev. D* **82** (2010) 051501 [1005.5365].
- [79] G. Bali, F. Bruckmann, G. Endrodi, Z. Fodor, S. Katz, S. Krieg et al., *The QCD phase diagram for external magnetic fields*, *JHEP* **02** (2012) 044 [1111.4956].
- [80] G. Bali, F. Bruckmann, G. Endrodi, Z. Fodor, S. Katz and A. Schafer, *QCD quark condensate in external magnetic fields*, *Phys. Rev. D* **86** (2012) 071502 [1206.4205].
- [81] I.A. Shovkovy, *Magnetic Catalysis: A Review*, vol. 871, pp. 13–49 (2013), DOI [1207.5081].
- [82] E.M. Ilgenfritz, M. Muller-Preussker, B. Petersson and A. Schreiber, *Magnetic catalysis (and inverse catalysis) at finite temperature in two-color lattice QCD*, *Phys. Rev. D* **89** (2014) 054512 [1310.7876].

- [83] V. Bornyakov, P. Buividovich, N. Cundy, O. Kochetkov and A. Schäfer, *Deconfinement transition in two-flavor lattice QCD with dynamical overlap fermions in an external magnetic field*, *Phys. Rev. D* **90** (2014) 034501 [[1312.5628](#)].
- [84] G. Bali, F. Bruckmann, G. Endrödi, S. Katz and A. Schäfer, *The QCD equation of state in background magnetic fields*, *JHEP* **08** (2014) 177 [[1406.0269](#)].
- [85] G. Endrodi, M. Giordano, S.D. Katz, T. Kovács and F. Pittler, *Magnetic catalysis and inverse catalysis for heavy pions*, *JHEP* **07** (2019) 007 [[1904.10296](#)].
- [86] A. Tomiya, H.-T. Ding, X.-D. Wang, Y. Zhang, S. Mukherjee and C. Schmidt, *Phase structure of three flavor QCD in external magnetic fields using HISQ fermions*, *PoS LATTICE2018* (2019) 163 [[1904.01276](#)].
- [87] H.-T. Ding, S.-T. Li, A. Tomiya, X.-D. Wang and Y. Zhang, *Chiral properties of (2+1)-flavor QCD in strong magnetic fields at zero temperature*, [2008.00493](#).
- [88] M. D’Elia, F. Manigrasso, F. Negro and F. Sanfilippo, *QCD phase diagram in a magnetic background for different values of the pion mass*, *Phys. Rev. D* **98** (2018) 054509 [[1808.07008](#)].
- [89] V.V. Braguta, A.Y. Kotov, D.D. Kuznedev and A.A. Roenko, *Lattice study of the confinement/deconfinement transition in rotating gluodynamics*, in *38th International Symposium on Lattice Field Theory*, 10, 2021 [[2110.12302](#)].
- [90] N.Y. Astrakhantsev, V.V. Braguta, N.V. Kolomojets, A.Y. Kotov and A.A. Roenko, *Equation of State of dense QCD in external magnetic field*, in *38th International Symposium on Lattice Field Theory*, 12, 2021 [[2112.01032](#)].
- [91] M. D’Elia, L. Maio, F. Sanfilippo and A. Stanzione, *Phase diagram of QCD in a magnetic background*, [2111.11237](#).
- [92] L.M.M.C.M.D. Alfredo Stanzione, Francesco Sanfilippo, “Lattice qcd in strong magnetic background.” Talk at Lattice 2021, 2021.
- [93] B.B. Brandt, F. Cuteri, G. Endrödi, G. Markó and A.D.M. Valois, *Lattice QCD with an inhomogeneous magnetic field background*, in *38th International Symposium on Lattice Field Theory*, 11, 2021 [[2111.13100](#)].
- [94] S.L.X.W.Y.Z. Akio Tomiya, Heng-Tong Ding, “Chiral properties of (2+1)-flavor qcd in background magnetic fields at zero temperature.” Talk Lattice 2021, 2021.
- [95] H.T. Ding, S.T. Li, Q. Shi and X.D. Wang, *Fluctuations and correlations of net baryon number, electric charge and strangeness in a background magnetic field*, *Eur. Phys. J. A* **57** (2021) 202 [[2104.06843](#)].
- [96] S.L.X.W. Heng-Tong Ding, Qi Shi, “Fluctuations and correlations of net baryon number, electric charge and strangeness in a background magnetic field.” Talk at Lattice 2021, 2021.

- [97] V. Braguta, M. Chernodub, A.Y. Kotov, A. Molochkov and A. Nikolaev, *Finite-density QCD transition in a magnetic background field*, *Phys. Rev. D* **100** (2019) 114503 [1909.09547].
- [98] BNL-BIELEFELD collaboration, *Baryon number and charge fluctuations from lattice QCD*, *Nucl. Phys. A* **904-905** (2013) 865c [1212.4278].
- [99] M. D'Elia, G. Gagliardi and F. Sanfilippo, *Higher order quark number fluctuations via imaginary chemical potentials in $N_f = 2 + 1$ QCD*, *Phys. Rev.* **D95** (2017) 094503 [1611.08285].
- [100] A. Bazavov et al., *The QCD Equation of State to $O(\mu_B^6)$ from Lattice QCD*, *Phys. Rev.* **D95** (2017) 054504 [1701.04325].
- [101] S. Borsanyi, Z. Fodor, J.N. Guenther, S.K. Katz, K.K. Szabo, A. Pasztor et al., *Higher order fluctuations and correlations of conserved charges from lattice QCD*, **1805.04445**.
- [102] A. Bazavov et al., *Skewness, kurtosis, and the fifth and sixth order cumulants of net baryon-number distributions from lattice QCD confront high-statistics STAR data*, *Phys. Rev. D* **101** (2020) 074502 [2001.08530].
- [103] D. Bollweg, J. Goswami, O. Kaczmarek, F. Karsch, S. Mukherjee, P. Petreczky et al., *Second order cumulants of conserved charge fluctuations revisited I. Vanishing chemical potentials*, **2107.10011**.
- [104] PARTICLE DATA GROUP collaboration, *Review of Particle Physics*, *PTEP* **2020** (2020) 083C01.
- [105] R. Bellwied, S. Borsanyi, Z. Fodor, J.N. Guenther, S.D. Katz, P. Parotto et al., *Corrections to the hadron resonance gas from lattice QCD and their effect on fluctuation-ratios at finite density*, **2102.06625**.
- [106] R. Bellwied, S. Borsanyi, Z. Fodor, J.N. Guenther, S.D. Katz, P. Parotto et al., *Quantifying corrections to the hadron resonance gas with lattice QCD*, in *38th International Symposium on Lattice Field Theory*, 12, 2021 [2112.02402].
- [107] STAR collaboration, *Net-proton number fluctuations and the Quantum Chromodynamics critical point*, **2001.02852**.
- [108] STAR collaboration, *Measurement of the Sixth-Order Cumulant of Net-Proton Distributions in Au+Au Collisions from the STAR Experiment*, in *28th International Conference on Ultrarelativistic Nucleus-Nucleus Collisions*, 2, 2020 [2002.12505].
- [109] R. Bellwied, S. Borsanyi, Z. Fodor, J.N. Guenther, J. Noronha-Hostler, P. Parotto et al., *Off-diagonal correlators of conserved charges from lattice QCD and how to relate them to experiment*, *Phys. Rev. D* **101** (2020) 034506 [1910.14592].
- [110] STAR collaboration, *Collision Energy Dependence of Moments of Net-Kaon Multiplicity Distributions at RHIC*, *Phys. Lett. B* **785** (2018) 551 [1709.00773].

- [111] S. Borsányi, Z. Fodor, J.N. Guenther, R. Kara, S.D. Katz, P. Parotto et al., *Lattice QCD equation of state at finite chemical potential from an alternative expansion scheme*, *Phys. Rev. Lett.* **126** (2021) 232001 [2102.06660].
- [112] T. Lee and C.-N. Yang, *Statistical theory of equations of state and phase transitions. 2. Lattice gas and Ising model*, *Phys. Rev.* **87** (1952) 410.
- [113] M. Giordano, K. Kapas, S.D. Katz, D. Negradi and A. Pasztor, *Radius of convergence in lattice QCD at finite μ_B with rooted staggered fermions*, *Phys. Rev. D* **101** (2020) 074511 [1911.00043].
- [114] P. Dimopoulos, L. Dini, F. Di Renzo, J. Goswami, G. Nicotra, C. Schmidt et al., *A contribution to understanding the phase structure of strong interaction matter: Lee-Yang edge singularities from lattice QCD*, 2110.15933.
- [115] G. Nicotra, P. Dimopoulos, L. Dini, F. Di Renzo, J. Goswami, C. Schmidt et al., *Lee-Yang edge singularities in 2+1 flavor QCD with imaginary chemical potential*, in *38th International Symposium on Lattice Field Theory*, 11, 2021 [2111.05630].
- [116] M.A. Schindler, S.T. Schindler and M.C. Ogilvie, *Finite-density QCD, \mathcal{PT} symmetry, and dual algorithms*, in *38th International Symposium on Lattice Field Theory*, 10, 2021 [2110.14009].
- [117] M.A. Schindler, S.T. Schindler and M.C. Ogilvie, *Finite-density QCD, \mathcal{PT} symmetry, and exotic phases*, in *38th International Symposium on Lattice Field Theory*, 10, 2021 [2110.07761].
- [118] M.A. Schindler, S.T. Schindler and M.C. Ogilvie, *\mathcal{PT} symmetry, pattern formation, and finite-density QCD*, 6, 2021, DOI [2106.07092].
- [119] M.E. Caplan and C.J. Horowitz, *Colloquium : Astromaterial science and nuclear pasta*, *Rev. Mod. Phys.* **89** (2017) 041002 [1606.03646].
- [120] W.-j. Fu, J.M. Pawłowski and F. Rennecke, *Strangeness Neutrality and QCD Thermodynamics*, *SciPost Phys. Core* **2** (2020) 002 [1808.00410].
- [121] W.-j. Fu, J.M. Pawłowski and F. Rennecke, *QCD phase structure at finite temperature and density*, *Phys. Rev. D* **101** (2020) 054032 [1909.02991].
- [122] M. Leonhardt, M. Pospiech, B. Schallmo, J. Braun, C. Drischler, K. Hebeler et al., *Symmetric nuclear matter from the strong interaction*, *Phys. Rev. Lett.* **125** (2020) 142502 [1907.05814].
- [123] J. Braun, M. Leonhardt and M. Pospiech, *Fierz-complete NJL model study III: Emergence from quark-gluon dynamics*, *Phys. Rev. D* **101** (2020) 036004 [1909.06298].
- [124] J. Braun, W.-j. Fu, J.M. Pawłowski, F. Rennecke, D. Rosenblüh and S. Yin, *Chiral susceptibility in (2+1)-flavor QCD*, *Phys. Rev. D* **102** (2020) 056010 [2003.13112].

- [125] N. Dupuis, L. Canet, A. Eichhorn, W. Metzner, J.M. Pawłowski, M. Tissier et al., *The nonperturbative functional renormalization group and its applications*, *Phys. Rept.* **910** (2021) 1 [2006.04853].
- [126] C.D. Roberts and S.M. Schmidt, *Dyson-Schwinger equations: Density, temperature and continuum strong QCD*, *Prog. Part. Nucl. Phys.* **45** (2000) S1 [nucl-th/0005064].
- [127] C.S. Fischer, J. Luecker and C.A. Welzbacher, *Phase structure of three and four flavor QCD*, *Phys. Rev. D* **90** (2014) 034022 [1405.4762].
- [128] F. Gao and Y.-x. Liu, *QCD phase transitions via a refined truncation of Dyson-Schwinger equations*, *Phys. Rev. D* **94** (2016) 076009 [1607.01675].
- [129] F. Gao and J.M. Pawłowski, *QCD phase structure from functional methods*, *Phys. Rev. D* **102** (2020) 034027 [2002.07500].
- [130] C.S. Fischer, *QCD at finite temperature and chemical potential from Dyson-Schwinger equations*, *Prog. Part. Nucl. Phys.* **105** (2019) 1 [1810.12938].
- [131] T.R. Morris, *The Exact renormalization group and approximate solutions*, *Int. J. Mod. Phys. A* **9** (1994) 2411 [hep-ph/9308265].
- [132] C. Fischer, “The qcd phase diagram with functional methods, lecture-2.” Talk at NA7-Hf-QGP, 2021.
- [133] P.J. Gunkel and C.S. Fischer, *Masses and decay constants of (axial-)vector mesons at finite chemical potential*, *Eur. Phys. J. A* **57** (2021) 147 [2012.01957].
- [134] C.S. Fischer, J. Luecker and C.A. Welzbacher, *Locating the critical end point of QCD*, *Nucl. Phys. A* **931** (2014) 774 [1410.0124].
- [135] F. Gao and J.M. Pawłowski, *Chiral phase structure and critical end point in QCD*, *Phys. Lett. B* **820** (2021) 136584 [2010.13705].
- [136] A. Chabane and G. Endrödi, *Roberge-Weiss transitions at imaginary isospin chemical potential*, 2110.13536.
- [137] F. Cuteri, A. D’Ambrosio, O. Philipsen and A. Sciarra, *The chiral phase transition from strong to weak coupling*, in *38th International Symposium on Lattice Field Theory*, 12, 2021 [2112.10429].
- [138] B.B. Brandt, F. Cuteri and G. Endrodi, *QCD thermodynamics at non-zero isospin asymmetry*, in *38th International Symposium on Lattice Field Theory*, 10, 2021 [2110.14750].